Development of Alumina-Forming Austenitic Stainless Steels

Yukinori Yamamoto
Oak Ridge National Laboratory, Oak Ridge, TN 37831-6115
yamamotoy@ornl.gov; Tel: (865) 576-7095; FAX (865) 576-6298

Michael P. Brady (corresponding author)
Oak Ridge National Laboratory, Oak Ridge, TN 37831-6115
bradymp@ornl.gov; Tel: (865) 574-5153; FAX (865) 241-0215

Michael L. Santella
Oak Ridge National Laboratory, Oak Ridge, TN 37831-6115
santellaml@ornl.gov; Tel: (865) 574-4805; FAX (865) 574-4928

Hongbin Bei
Oak Ridge National Laboratory, Oak Ridge, TN 37831-6115
beih@ornl.gov; Tel: (865) 576-7196; FAX (865) 574-7659

Philip J. Maziasz
Oak Ridge National Laboratory, Oak Ridge, TN 37831-6115
maziaszpj@ornl.gov; Tel: (865) 574-5082; FAX (865) 574-7659

Bruce A. Pint
Oak Ridge National Laboratory, Oak Ridge, TN 37831-6156
pintba@ornl.gov; Tel: (865) 576-2897; FAX (865) 241-0215

ABSTRACT

Work in fiscal year 2008 focused on the development of creep-resistant, alumina-forming austenitic (AFA) stainless steel alloys, which exhibit a unique combination of excellent oxidation resistance via protective alumina (Al_2O_3) scale formation and high-temperature creep strength through the formation of stable nano-scale MC-type carbides [1-8]. Levels of Nb additions(> 1 wt.% Nb and/or Ni additions in the range of ~25-30 wt.% and Al levels of 2.5-4 wt.%, were found to correlate with an increase in the upper-temperature limit for Al_2O_3 scale formation in air (~900°C) and air with 10% water vapor (~800°C). Creep resistance also showed a strong dependence on the level of Nb additions, and was correlated with volume fraction of MC-type carbides using thermodynamic computational tools. A ~50 lb trial heat of a AFA alloy ingot was made using conventional single-melt vacuum techniques, and that alloy was successfully hot-rolled without any cracking [2]. This heat showed good weldability using matching filler material of the same alloy.

INTRODUCTION

High-temperature oxidation resistance results from the establishment of a continuous protective oxide layer. Virtually all Fe-rich heat-resistant stainless steels (made by conventional cast/forging technology) rely on chromia (Cr_2O_3) scales for oxidation protection above ~600°C. Alumina (Al_2O_3) scales grow at a slower rate [9-16] and are more stable in water-vapor containing environments than chromia scales. This latter factor is a key advantage, as water vapor significantly accelerates the oxidation rate of chromia-

forming stainless steels [11] at the levels encountered in virtually all combustion environments. However, the strong body-centered cubic (BCC) stabilizing effect of Al makes it difficult to develop austenitic (face centered cubic) stainless steels capable of alumina scale formation [3]. Alumina-forming, ferritic steels such as FeCrAl-based alloys are available but are too weak to be used as structural alloys above ~500-600°C unless strengthened by oxide dispersions using expensive powder metallurgical consolidation approaches. Creep-resistant, alumina-forming Ni-base alloys are also available, but are also too costly for many applications.

Recent efforts at Oak Ridge National Laboratory have identified austenitic alloy composition ranges that have the potential for both creep-resistance and alumina scale formation in the 600-900°C temperature range [1-8], at estimated alloy raw material cost comparable to existing advanced austenitic stainless steel families. Components of interest range from super-heater tubes in steam boilers to gas-to-gas heat exchangers and hot-section gas-turbine components, with potentially higher operating temperatures and increased environmental durability compared to conventional chromia (Cr_2O_3)-forming stainless steels and Ni-base alloys.

DISCUSSION OF CURRENT ACTIVITIES

Efforts in fiscal year (FY) 2008 focused on evaluation of the oxidation resistance and mechanical properties of a range of developmental AFA alloy compositions (Table 1). In the Table all alumina-forming austenitic (AFA) compositions (2.5, 3, and 4 wt% Al developmental series) were adjusted to yield an austenitic matrix structure based on experimental findings and computational thermodynamic modeling.

Table 1- Listing of the nominal compositions of select alloys investigated to date (details available in references 2-8).

Alloy Designation	Nominal Composition (wt%, balance Fe)													
	Ni	Cr	Al	Nb	Ti	V	Mo	W	Cu	Mn	Si	C	B	P
Initial Creep-Resistant, Alumina-Forming Austenitic Alloy														
AFA 2-1	20	14.3	2.5	0.9			2.5			2	0.15	0.08	0.01	0.04
2.5 wt% Al series														
AFA 2-2	20	14.3	2.5	0.16	0.1	0.1	2.5			2	0.15	0.08	0.01	0.04
AFA 2-3	20	14.3	2.5	0.16			2.5			2	0.15	0.08	0.01	0.04
AFA 2-4	21	14	2.5	3		0.18	3.4					0.02	0.02	
AFA 2-5	21	14	2.5	3.3			3.4					0.08	0.08	
3 wt% Al series														
AFA 3-1	20	14.3	3	0.4	0.1		2	1	0.5	2	0.15	0.08	0.01	0.04
AFA 3-2	20	14.3	3	0.6	0.1		2	1	0.5	2	0.15	0.1	0.01	0.04
AFA 3-3	26	14	3	0.6			1.25			0.2	0.2	0.04	0.01	0.015
AFA 3-4	20	14.3	3	1			2	1	0.5	2	0.15	0.1	0.01	0.02
AFA 3-5	20	14.3	3	1		0.2	2	1	0.5	2	0.15	0.1	0.01	0.02
AFA 3-7	20	14.3	3	1.5	0.1		2	1	0.5	2	0.15	0.1	0.01	0.04
AFA 3-8	20	14.3	3	2.5	0.1		2	1	0.5	2	0.15	0.1	0.01	0.04
4 wt% Al series														
AFA 4-1	20	12	4	0.6	0.1		2	1	0.5	2	0.15	0.1	0.01	0.04
AFA 4-2	20	12	4	1			2	1	0.5	2	0.15	0.1	0.01	0.02

OXIDATION RESISTANCE

Alumina scale formation by AFA alloys was initially demonstrated by 1000 h exposures in air and in air + 10% water vapor environments at 650 and 800 ^{o}C [3]. The AFA alloy compositions developed to date do not appear to be as "strongly alumina-forming" as conventional FeCrAl and Ni-base alloys, which is a consequence of the need to balance mechanical properties and weldability with oxidation resistance in the AFA alloy range. Excellent oxidation resistance in air and air with 10% water vapor at 650 and 700°C has been observed thus far (sample exposures up to 5000-6000 h). However, at 800°C in air with 10% water vapor and at 900 ^{o}C in dry air, many of the AFA compositions become susceptible to internal oxidation of Al, and lost their capability to form external alumina scales [5,7]. None of the current compositions formed protective alumina scales at 1000°C in air. This loss of oxidation resistance is illustrated in Fig. 1 for alloy AFA 3-7 (3Al/1.5Nb/0.1Ti) and alloy AFA 2-4 (2.5Al/3Nb/0.2V). Alloy AFA 3-7 showed excellent oxidation resistance at 800 and 900°C in air, but was significantly degraded at 800°C in air with 10% water vapor. Alloy AFA 2-4 also exhibited excellent oxidation resistance at 800°C in air. At 800°C in air with 10% water vapor, AFA 2-4 exhibited good resistance to 4500 h of exposure, but then exhibited a transition to the formation of Fe-base oxide nodules. At 900°C in air, alloy AFA 2-4 exhibited poor oxidation resistance. The loss of protective oxidation behavior was associated with a transition to internal oxidation and nitridation of Al [7].

Figure 2 presents plots where alumina scale formation is possible as a function of Al and Nb content. Compositions above the boundary lines (estimated) exhibit protective alumina scale formation based on ~1000-6000 h exposures. It should be noted that the 3Al-2.5Nb alloy exposed in air with 10% water vapor at 800°C showed a transition to nodule formation at 5300 h, such that ongoing studies will likely result in a further shift to the right of this estimated alumina formation boundary line. The amount of Al and Nb needed for alumina scale formation increased moderately from 800 to 900°C (Fig. 2a). Increasing the alloy Ni level from 20 to 26 wt% decreased the amount of Nb needed for alumina scale formation at 900 ^{o}C in air. In air with 10% water vapor at 800°C, high Nb (2.5-3 wt%) rather than high Al correlated with protective alumina scale formation (Fig. 2b). High levels of Ni (32 wt%) also decreased the lower limit of the Al addition needed to form and maintain alumina formation in the presence of water vapor. The mechanisms behind these trends are not yet understood and are the subject of ongoing investigation. It is speculated that oxygen solubility is a key factor, with increased Nb level possibly reducing oxygen solubility, which would favor external alumina scale formation [2].
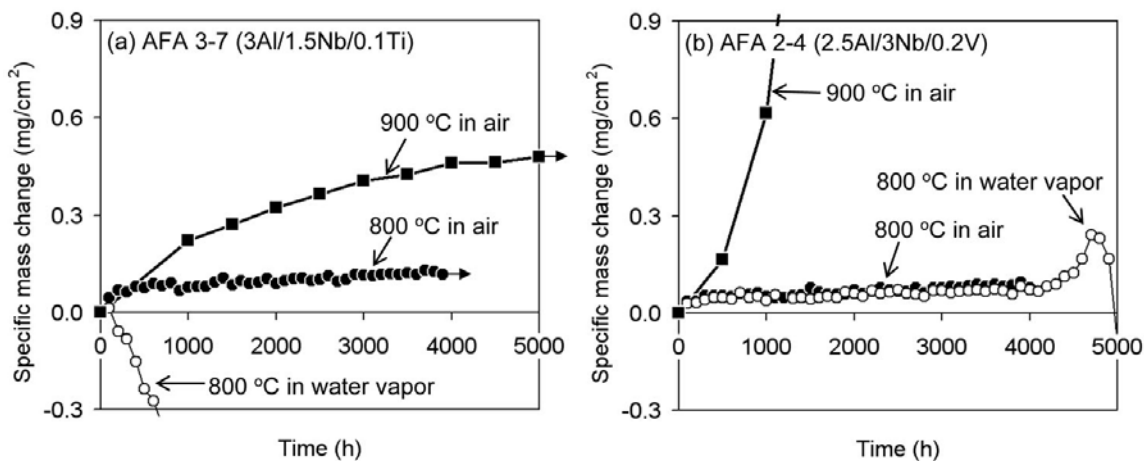

Fig. 1-Oxidation kinetics at 800/ 900 °C in air or in air with 10% water vapor: (a) AFA 3-7, and (b) AFA 2-4 (after reference 7).

The solubility of Al in the austenitic matrix is on the order of ~2 to 2.5 wt% Al, so that the higher-Al containing alloys, such as the alloys with 3 or 4 wt% Al, exhibit second phase dispersions of B2 (Ni,Fe)Al during aging [7,8]. These precipitates act as Al reservoirs for the growth of alumina scales [7], resulting in a B2-denuded zone directly underneath the scale (Fig. 3). The Al concentration profile within the B2-denuded zone for the 3 and 4 wt% Al alloys examined to date remained constant near the solubility limit of Al in the austenitic matrix (~2-2.5 wt.%). The alloy AFA 2-4 (2.5Al/3Nb/0.2V) showed evidence of significant subscale Al depletion when oxidized at 900°C in air, which is considered the reason for the loss of alumina scale formation (Fig. 1b) [7]. Therefore, a minimum of 3 wt% Al in the alloy appears sufficient to maintain alumina scale formation in the 800-900°C range, assuming with sufficient Nb addition.
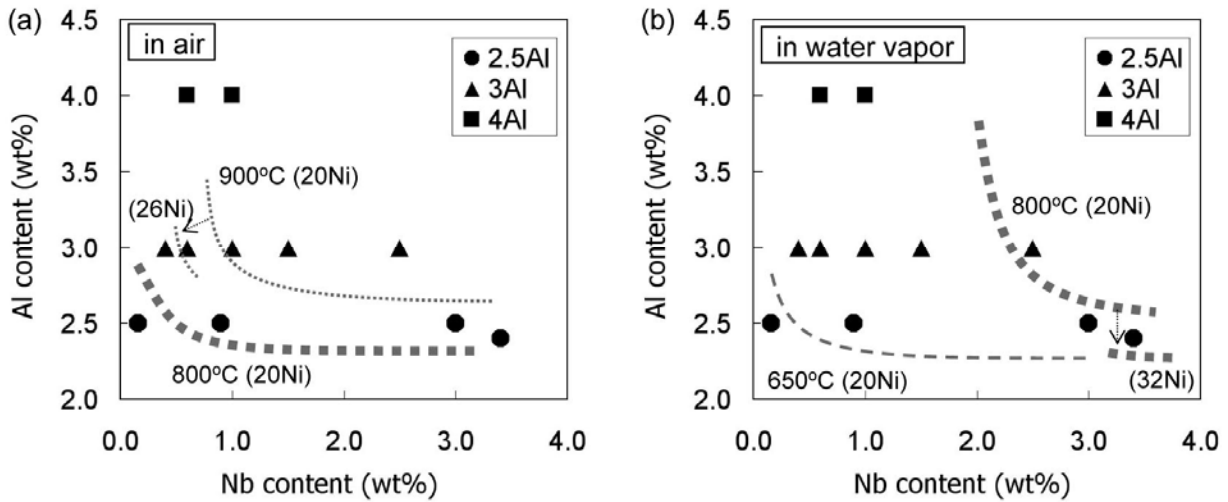

Fig. 2- Composition maps of alumina formation as a function of Al and Nb level in (a) air and (b) air with 10% water vapor.
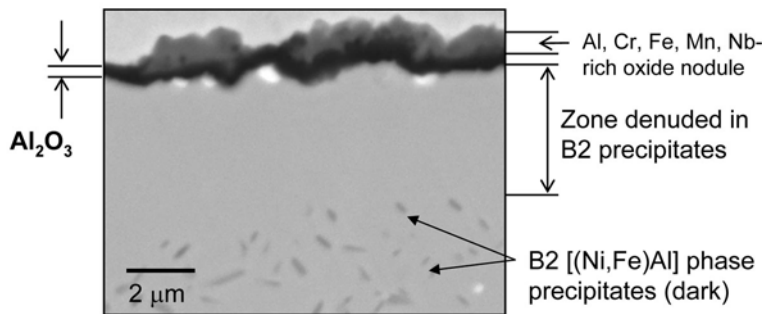

Fig. 3- Backscattered electron image of AFA 4-1 (4Al/0.6Nb/0.1Ti) after 100 h at 900 °C in air (after reference 7).

HIGH-TEMPERATURE CREEP PROPERTIES

Creep-rupture life testing of the AFA alloys was conducted at 750-850°C and 70-170 MPa in air using a sub-sized dogbone tensile specimen configuration suitable for screening evaluation purposes [1-4, 6, 8]. The 170 MPa stress levels were used as an accelerated screening protocol to provide rapid feedback on the effects of alloy composition trends on creep resistance. Figure 4 shows a Larson-Miller parameter plot of the AFA alloys and select commercial heat-resistant steel alloys [18-20]. The data for the AFA

4

alloys indicates excellent creep resistance, comparable to those of state-of-art heat-resistant austenitic stainless steels such as alloy 709 (Fe-20Cr-25Ni base), and approaching the range of the Ni-base alloy 617 (Ni-20Cr-10Co-8Mo base).
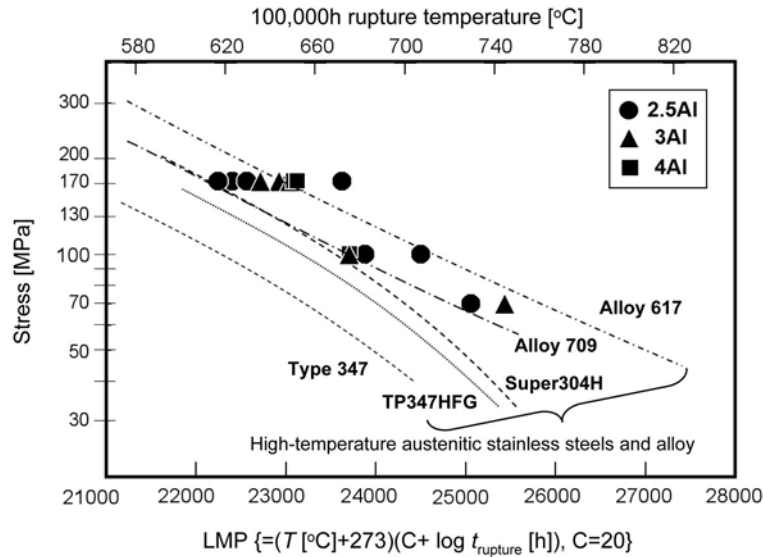

Fig. 4- Larson Miller parameter plots of the AFA alloys creep-rupture tested at 750 – 850 °C, together with those of heat-resistant austenitic steel alloys (after reference 1-4, 6, 8, 18-20).
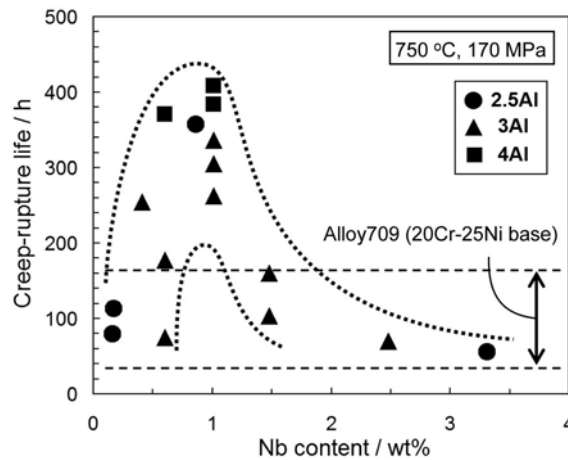

Fig. 5- Creep-rupture life data for the AFA alloys at 750 °C and 170 MPa in air plotted as a function of the Nb content (after reference 8). The dashed lines correspond to the creep-rupture of alloy 709 (no prior cold work) extrapolated to these test conditions [22].

The creep resistance of the AFA alloys was strongly dependent on Nb content. Figure 5 shows creep-rupture life data at 750°C and 170 MPa for a range of AFA alloys as a function of the Nb content (50 – 150 μm range grain sizes) [8]. All specimens were tested in the solution heat-treated condition with 10% cold-work in order to promote the nucleation of nano-scale MC-type carbides for high creep resistance [18, 19]. Maximum creep-rupture lives were observed at around 1 wt% Nb, which were slightly longer than the extrapolated life for alloy 709 (50 – 150 h [22]) under these conditions. The maximum creep-rupture lifetime was independent of the Al level in the range of 2.5 – 4 wt% for the AFA alloys examined.

5

Microstructural analysis of creep-ruptured specimens revealed dense dispersions of (Ni,Fe)Al-type B2 phase and $Fe_2(Mo,Nb)$-type Laves phase in the 300 nm size range, as shown in Fig. 6a. for alloy AFA 3-2 (3Al/0.6Nb/0.1Ti). Nano-scale MC-type carbides were observed in the austenite matrix (Fig. 6b), and are considered to be the primary source of the excellent creep resistance of these alloys. The amount of B2 phase increased significantly with increasing levels of Al additions. The higher Nb levels also correspondingly resulted in higher quantities of Laves phase precipitates, although these precipitates did not correlate with improved creep resistance. Preliminary computational thermodynamic calculations predicted that the amount of MC would exhibit a maximum around 1 wt% Nb, which is consistent with the creep-rupture life trends observed [8]. The calculations also predicted that for the 4Al wt% alloys, MC-type carbide formation (and possibly creep resistance) would peak at around ~1.5 wt% Nb [8]. Alloy preparation and creep evaluations to test this prediction are planned.
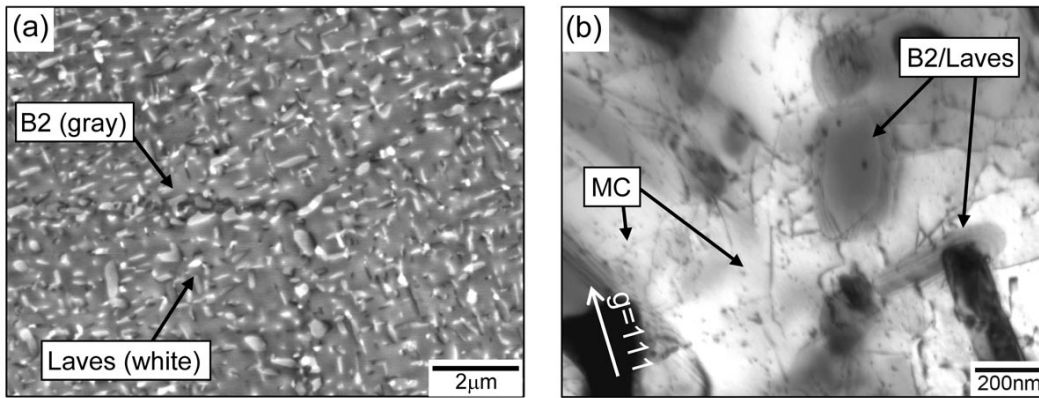

Fig. 6- Microstructure of creep-ruptured AFA 3-2 (3Al/0.6Nb/0.1Ti) tested at 750 ^{o}C and 170 MPa: (a) SEM back-scattered electron image and (b) TEM bright field image.

TENSILE PROPERTIES

Tensile properties of select AFA alloys in the solution heat-treated condition are shown in Table 2. Little variation as a function of alloy composition was evident. The room-temperature yield strength was ~250 MPa, with yield strength remaining above 200 MPa at 750°C and above 170 MPa at 850°C. The tensile elongation was ~50% at room temperature, with a decrease to the 30-40% range between 650 - 750 ^{o}C. It is speculated that this ductility reduction results from precipitation of B2, Laves, and MC phases, although necking due to plastic instability also may play a major role. The observed tensile behavior was similar to that of commercial heat-resistant austenitic stainless steels [2,8], which suggests that the Al additions do not degrade the mechanical properties (at least in the solution treated condition). Further study of this issue is planned.

WELDABILITY

A 50 lb trial heat of AFA 4-1 was made by an industrial collaborator using conventional single-melt vacuum techniques, and the alloy was successfully hot-rolled without any cracking. The weldability of AFA 4-1 plate was screened using gas tungsten arc welding with matching weld filler. Figure 7 shows the macro- and microstructure of the welded plate. A preliminary evaluation indicated that no cracking had occurred, either in the fusion zone or the heat-affected zone (Fig. 7c). A similar weldability screening conducted for AFA 2-1 [1,3] also showed no cracking after gas tungsten arc welding. Therefore, it appears that the AFA alloys may be amenable to conventional welding processes.

6

Table 2- Tensile properties of the AFA alloys at room and elevated temperatures (after reference 8).

Name	Remarks	Temperature (^{o}C)	*YS (MPa)	*UTS (MPa)	Elongation (%)
AFA 2-1	*GS: 74 μm, 10% cold-worked	20	523	650	22
		750	349	407	26
AFA 3-4	GS: 55 μm	20	261	613	51
		750	201	357	32
AFA 4-1	GS: 28μm	20	282	660	50
		650	237	491	45
		750	226	321	42
		850	172	182	51
	GS: 64 + 300 μm, (Bi-modal GS)	20	256	595	54
		650	199	479	50
		750	212	357	36
		850	173	186	33
AFA 4-2	GS: 50 μm	20	268	644	49
		750	232	373	39

*YS: yield strength; UTS: ultimate tensile strength; GS: Grain size.
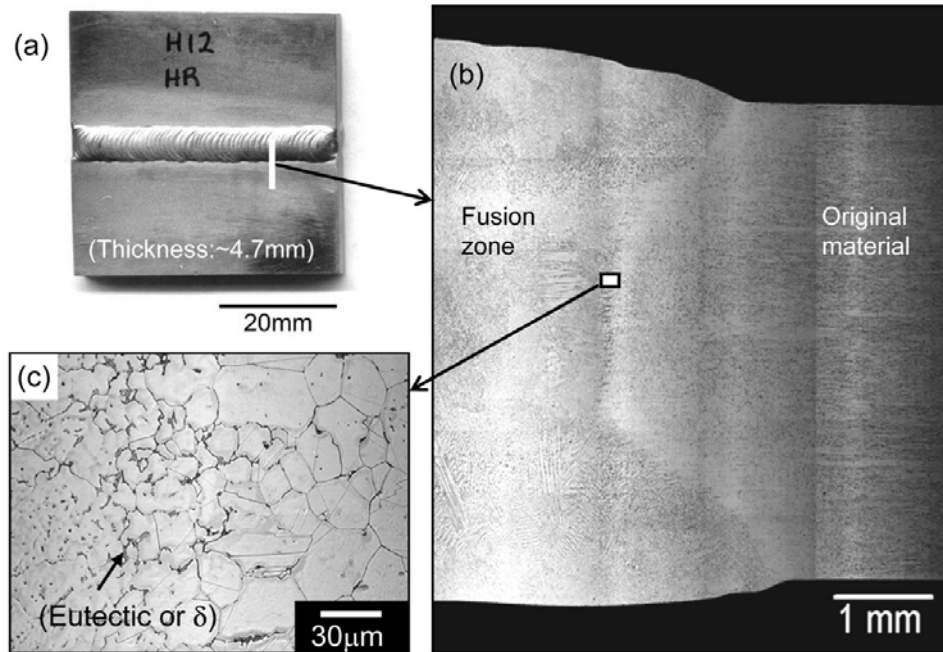

Fig. 7- Weldability screening of vacuum cast and hot-rolled AFA 4-1 (4Al/0.6Nb/0.1Ti) by gas tungsten arc welding using AFA 4-1 filler (after reference 2): (a) overall view, and (b and c) optical micrographs of cross-sections.

CONCLUDING REMARKS

The AFA alloys developed to date show a promising combination of creep resistance, oxidation resistance, tensile properties, as well as the potential for good welding behavior. These results suggest that the optimum alloy composition is in the range of Fe-(20-25)Ni-(12-15)Cr-(3-4)Al-(1-3)Nb wt% base, with higher Nb levels favored for more aggressive oxidizing conditions (e.g. water vapor) and lower Nb levels favored for applications requiring optimum creep resistance [2]. The properties achieved to date are

considered to be sufficient to merit evaluation for industrial applications up to ~700-750 $^{\circ}$C. Additional alloy development will be needed for higher-temperature applications (~750-900 $^{\circ}$C). The key challenge will be to further optimize the ability to form an alumina scale, without sacrificing mechanical properties and weldability. To achieve this, a better understanding of the role of minor alloying additions in promoting or degrading alumina scale formation is needed, particularly Al, Cr, Nb, Ni, Ti, and V. Study of this issue will be a priority for FY 2009 work.

ACKNOWLEDGEMENTS

REFERENCES

1. M.P. Brady, Y. Yamamoto, Z.P. Lu, P.J. Maziasz, C.T. Liu, B.A. Pint, and M.L. Santella, Stainless Steel World Magazine, March 2008.
2. M.P. Brady, Y. Yamamoto, M.L. Santella, P.J. Maziasz, B.A. Pint, C.T. Liu, JOM, 60 (7), pp. 12-18, 2008.
3. Y. Yamamoto, M. P. Brady, Z. P. Lu, P. J. Maziasz, C.T. Liu, B.A. Pint, K.L. More, H.M. Meyer, E.A. Payzant, Science, Vol. 316, no. 5823 (2007), pp. 433-436.
4. Y. Yamamoto, M.P. Brady, Z. P. Lu, C. T. Liu, M. Takeyama, P. J. Maziasz, and B. A. Pint, Met. Mater. Trans. 38A, 11 (2007), pp. 2737-2746.
5. M.P. Brady, Y. Yamamoto, M.L. Santella, B.A. Pint, Scripta Mater 57, 12 (2007), pp. 1117-1120.
6. Y. Yamamoto, M. Takeyama, Z.P. Lu, C.T. Liu, N.D. Evans, P.J. Maziasz, and M.P. Brady, Intermetallics, 16, 3 (2008) pp. 453-462.
7. M.P. Brady, Y. Yamamoto, B.A. Pint, M.L. Santella, P.J. Maziasz, and L.R. Walker, Materials Science Forum Dec 2008 (in press).
8. Y. Yamamoto, M.L. Santella, M.P. Brady, H. Bei, C. T. Liu, and P.J. Maziasz, to be submitted (2008).
9. G.Y. Lai, "High Temperature Corrosion of Engineering Alloys", ASM International, Materials Park, OH (1990)
10. B. Gleeson, in "Corrosion and Environmental Degradation", Volume II, M. Schutze, Ed., Materials Science and Technology Series, Wiley-VCH, Weinheim, Germany, chapter 5, pp. 173-228 (2000).
11. P. Kofstad, Ed., High Temperature Corrosion, (Elsevier, London, 1988).
12. M.P. Brady, B.A. Pint, P.F. Tortorelli, I. G. Wright, and R. J. Hanrahan, Jr., in "Corrosion and Environmental Degradation", Volume II, M. Schutze, Ed., Materials Science and Technology Series, Wiley-VCH, Weinheim, Germany, chapter 6, pp. 229-325 (2000).
13. J. Doychak, in: "Intermetallic Compounds: Principles and Practice Vol. 1", J.H. Westbrook, R.L. Fleischer (Eds.), New York: John Wiley & Sons, pp. 977-1016 (1994).
14. G.H. Meier, Materials and Corrosion, 47 (11), pp. 595-618 (1996).
15. G. Welsch, J.L. Smialek, J. Doychak, J. Waldman, N.S. Jacobson, in: Oxidation and Corrosion of Intermetallic Alloys, G. Welsch, P.D. Desai (Eds.), West Lafayette, IN: Purdue Research Foundation, pp. 121-266 (1996).
16. G.J. Yurek, in:"Corrosion Mechanisms", F.Mansfeld (Ed.), New York: Marcel Dekker, Inc., pp. 398-446 (1987).
17. F.G. Wilson, B.R. Knott, C.D. Desforges, Met Mater Trans A, 9, 2, pp. 275-282 (1978).
18. R. W. Swindeman, P. J. Maziasz, E. Bolling, J. F. King, Oak Ridge Natl. Lab. Rep. ORNL-6629/P1, Oak Ridge, TN, 1990).
19. R. W. Swindeman and P. J. Maziasz: *Proc. of the 1st Int. Conf. on Heat-Resistant Materials*, K. Natesan and D. J. Tillack, eds., ASM International, Materials Park, OH, 1991, pp. 251-259.
20. J. P. Shingledecker, P. J. Maziasz, N. D. Evans, M. J. Pollard, Proc. ECCC Conference on Creep and Fracture in High Temperature Components Design and Life Assessment Issues, (DEStech, Lancaster, PA, 2005), pp. 99-109.
21. Allegheny Ludlum, *TECHNICAL DATA BLUE SHEET, Stainless Steels, types 321, 347 and 348*, (ATI Allegheny Ludlum Corp., Pittsburgh, PA, 2003; www.alleghenyludlum.com).
22. *Quality and Properties of NF709 Austenitic Stainless Steel for Boiler Tubing Applications*, Nippon Steel Corporation, Tokyo, Japan 1996.